BNL-64524
CONF-970517--

A STUDY OF THE BEHAVIOR OF BROMIDE IN ARTIFICIAL PITS USING *IN SITU* X-RAY MICROPROBE ANALYSIS

H. S. Isaacs+ and M. Kaneko*

+ Department of Applied Science,
Brookhaven National Laboratory, Upton NY 11973, USA..
**Nippon Steel Corp.,*
2-6-3 Otemachi Chiyoda-Ku,
Tokyo 100-71, Japan.

ABSTRACT

An *in situ* x-ray microprobe analysis of Type 316 stainless steel artificial pits has been carried out with bromide/chloride solution. A high intensity 8 μm diameter polychromatic x-ray beam was scanned across the steel/solution interface within the artificial pit. The resulting x-ray fluorescence was analyzed using an energy dispersive x-ray detector. In contrast to the light Cl atom, Br could be detected, making it possible to monitor the behavior of halides in the artificial pits and in the salt layer at the interface. It was found that Br was more active than Cl. At high potentials, elemental Br was produced as an oxidation product, whereas without added bromide, chloride only formed a salt layer. Br also concentrated at the salt/steel interface at potentials below where it was oxidized.

INTRODUCTION

Major changes in solution composition occurs when pits and pores are produced. It is the purpose of this paper is to describe an *in situ* x-ray fluorescence technique for solution analysis that has been used to measure changes taking place during pitting of stainless steels.(1,2) The technique has many similarities to scanning electron microprobe analysis, but uses x-rays rather than electrons, to excite the elements. The particular advantage of the technique was the in situ electrochemical control maintained during measurements. The technique offers a method for determining, in detail, the concentration or depletion of elements at the metal/solution interface with a sensitivity difficult to achieve using other techniques.

X-ray fluorescence has been used for many decades. (3,4) With the advent of light sources and high intensity x-rays, collimated beams, micrometers in size, have been developed for the spatial resolution of elemental distributions.(5) In this electrochemical study of artificial pits, bromide is introduced to test if it could be used to trace the behavior of chloride ions. Cl is a relatively light element with a low x-ray florescence energy that is too weak to penetrate about 0.25 mm of plastic used for windows in the cell construction. (1,2) This work demonstrated that there were limitations in attempting to substitute Br for Cl under conditions associated with pitting.

There have been few direct investigations of the solution in pits and cracks mainly owing to difficulties in analyzing the small volumes of solution involved (1,2,6-9). Consequently, few models take into consideration the importance of the solution chemistry

in pitting. Local changes in solution composition are the dominant factors in the initiation and propagation of pits in stainless steels (10-15). In contrast, many theories have been proposed for the breakdown of passivity but these are usually developed only up to the point where passivity is disrupted and assume that corrosion will continue because of active dissolution.(14-17) However, in most solutions under conditions where pitting can develop, surfaces generally repassivate following mechanical removal of the passive film. This indicates that disruption of passivity is not a sufficient requirement for localized corrosion to begin.

EXPERIMENTAL

In situ x-ray microprobe measurements of concentration gradients of species in artificial one-dimensional pits were made using foil electrodes about 0.015 mm thick (1,2). Fig. 1 shows a schematic of the electrochemical cells used to study effects of chemistry changes in pit solutions and at pit surfaces during metal dissolution in restricted geometries. The figure represents an artificial pit produced by dissolving back the cross section of a foil mounted between plastic sheets. The dissolving surface was under potentiostatic control. The original edge of the upward facing foil was in contact with a bulk solution in which a counter and saturated calomel reference electrode were placed. He bubbling stirred the bulk solution to maintain a zero dissolved metal ion concentration at the pit mouth. The foil/pit solution region was analyzed using x-ray fluorescence. High intensity polychromatic x-rays from beamline X26A at the National Synchrotron Light Source were collimated to produce a beam about 0.008 mm diameter. The intensity of the beam was generally attenuated by 0.150 mm Al foil. This was to reduce the formation of bubbles, probably hydrogen, when the beam passed over the metal/salt interface.

The x-ray beam was incident at 45° to the cell face. The energy dispersive detector was positioned at 45° to the sample surface and 90° to the incident beam. Kα fluorescence was counted to determine relative concentrations. The incident beam was scanned across the metal/solution interface by stepping the position of the cell in 0.001 mm steps. A live time of 5 s was used to acquire the x-ray data with real times ranging down from 6.6 to 5.7 s on stepping from over the steel to over the solution. Each scan took about 200 s. Fig. 2 is an example of an x-ray spectrum from a pit solution just above an Fe alloy with 20 Ni, 12 Cr, and 5 Mo with a bulk solution of 1M LiBr. The x-ray intensity for an element was taken as the area under the peak associated with that element.

The results presented were obtained with a 1M $LiCl_{0.75}Br_{0.25}$ bulk solution. The Type 316 stainless steel foil had a weight per cent composition of 0.028 P, 0.001 S, 16.41 Cr, 10.13 Ni, and 2.10 Mo.

RESULTS

When the steel surface was covered by a salt layer a potential step only gave a corresponding small perturbations in the current. The current soon attained its previous value and then continued its steady decrease with time as the pit deepened. Fig. 3 shows a plot of the potential changes and currents after the experiment had run for 7900 s. The pit depth was about 0.7 mm. When the potential was stepped from 2.2 to 2.6 V (all potential are referenced to a saturated calomel electrode) the current showed the expected small perturbations. However, on stepping to 3.0 V there was a significant change in behavior.

DISCLAIMER

The current stopped its steady decrease and began to increase. On increasing the potential to 3.4 V a major step in the current occurred and it became unpredictable. The increase in the current was associated with the formation of Br_2. Under the microscope Br_2 was first seen as red/brown semicircles radiating from sites on the metal surface. It then covered the dissolving edge of the steel surface and the adjacent pit solution. The changes at the interface were studied using x-ray microprobe.

The measured x-ray intensity was the convolution of the beam shape and a product of the "matrix effect" and the element concentration. The matrix effect depends on many factors, in particular, the atomic number, the concentration of each element, filters on the incoming beam, and filters on the detector.(2-4) The matrix effect changes with differences in chemical composition of the sample and incorporates interelement absorption and secondary fluorescence.(4)

The symbols in Fig. 4a are examples of measured intensity variations of Fe, Cr, and Br across the steel/solution interface and the ratio of the Fe/Cr intensities. The measurements were made when the applied potential was 2.6 V. The highest intensity was for Fe over the steel. The intensity decreased as the beam traversed the interface. In contrast to the results for Fe, the intensity of Cr, showed a smooth transition as the beam passed from the metal to the solution. In Fig. 4a a maximum, close to the interface, is observed in the Br results and occurs nearer to the metal surface than the maximum in the Fe/Cr ratio. The intensities have been deconvoluted using the variation in the Cr results across the metal interface to determine the shape of the x-ray beam. Fig. 4b shows the product of the concentration and the matrix effect. Future calculations are required to separate these two factors but the figure clearly shows the position of elements in the different phases. The fits of the calculated intensity were obtained by convolution of the beam shape and a model of the interface (Fig 4b). These are shown by the full lines in Fig. 4a. In addition, a component of these fits due to layers of materials adjacent to the metal surface, i.e. Fe_{SALT} and Br_{SALT}, are of particular interest and are therefore also presented in Fig. 4a. Similar procedures were adopted in Fig. 5.

The results in Fig. 4 show maxima for Br and the Fe/Cr ratio. The maximum for Fe/Cr ratio is further from the steel surface than the maximum in the Br results. The maximum for Fe/Cr ratio corresponded to the position of the knee in the Fe results. In Fig. 4b the step in the model of the interface is taken to correspond to Fe in the salt layer and spans 8 μm from the steel surface. Br at the steel interface spans 3 μm within the range of the iron in the salt layer indicating that Br has concentrated at the metal/salt interface. This is also shown by the convoluted Br_{SALT} curve that was closer to the metal and was not as wide as the Fe_{SALT} curve.

At a higher potential of 3.0 V, Fig 5a, a greater separation in the positions the maxima for the Br and Fe/Cr curves of about 3 μm was observed. In addition, a distinct maximum was observed in the Fe results in Fig. 5a. The presence of the dip in the Fe before the maximum was the important observation. It was a clear indication of a deficiency of Fe between the salt layer and the metal. No Ni, Mo, or Cr, the other major alloying elements in the steel showed any build-up in concentrations in this region and therefore, had not substituted for the Fe. The only corresponding increase was in Br.

DISCUSSION

It was expected that bromide, when added to chloride, would assist in the measurement of the salt at the interface including its thickness dependence on potential. An object of this study was also to determine how Br would substitute for Cl in the salt layer on the steel. High concentrations of halide, well above that in the bulk solution, are present in the pit because of high dissolution rates of the steel, transport of halide into the pit and a high solubility of metal halide salts. Some differences in the Cl/Br ratio from the bulk solution would be expected based on differences in the mobilities of the Cl and Br. Assuming that Br simply substitutes in direct proportion to its concentration in the saturated solution and the salt layer, the presence of Br in the salt would be detectable because of the higher density of the salt than the adjacent saturated solution. However, the observed behavior was found to be more complicated.

In experiments where breakdown did not occur, i.e. below 3 V, the current response was similar to that expected in chloride solutions. After a potential step the current showed a small transient but then returned to its value before the potential change. The presence of elevated amounts of Br at the metal/salt interface were predicted and were intended to offer delineation of the salt layer. It was previously shown that very low concentrations of Cr were present at the metal interface and the thickness of the Cr deficient layer increased with potential. (1,2) It was assumed that the thickness of the depleted layer represented the thickness of the salt layer. The distinct maximum in the ratio of Fe to Cr intensity at the metal/solution interface is again seen in Figs. 4a and 5a. In Fig. 4a a maximum is also observed in the Br curve close to the interface. The maximum occurs at a position slightly closer to the metal than the maximum in the curve of the Fe/Cr ratio. The difference in the maximum positions was about 2 μm. In general, for similar experiments with different stainless steels and bromide to chloride additions, a maximum in Br occurs closer to the interface than the maximum in the Fe/Cr ratio. These results indicate the salt layer on the steel is non-uniform. At the metal surface the Fe/Cr ratio is similar to the steel and there is a high Br concentration. On the saturated solution side of the salt layer, a Cr depleted region is formed with a Br concentration similar to the solution. It is possible that Br was the cause of the non-uniformity, but impedance studies with chloride alone, are consistent with a salt layer having an outer porous and inner compact layer. (18)

In previous experiments with only chloride present and high applied voltages of 4.0 V, (1) thick salt layers were formed without changes in the electrochemical behavior. Step increases in potential produced only transitory increases in current as the salt layer thickened (19- 21). From a purely thermodynamic viewpoint, the high electronegativity elements are predicted to form O_2, Cl_2 and Br_2 at potentials above about 1 V at a pH=0 (22) expected in these pits. In practice, however, the oxidation does not take place within pits when only chloride solutions are used. This was the expected behavior because the potential drop across the salt layer increased linearly with potential leaving a fixed but low potential at the salt/steel interface.(21) From thermodynamic data Br_2 formation is expected at a potential only about 0.1 V less positive than oxidation to form Cl_2.(22) Hence, a similar behavior at high voltages appeared possible with bromide present. However, Br_2 formation did occur when the potential was raised above 3 V. Under these conditions rapid metal dissolution would be expected suggesting another surface film, possibly a conducting oxide, had formed that did not inhibited Br_2 production. A somewhat similar behavior has been observed with Ti in bromide solutions. (23)

Measurements at 3.0 V showed distinct changes from those observed at lower voltages were taking place. There was a distinct decrease in the Fe component at the interface and an increase in Br as shown in Figure 5a. A similar behavior of Fe has not been observed in only choride solutions. The decrease in the Fe was not compensated by any increase in Ni, Cr or Mo. This behavior suggested that a Br_2 phase had formed separating the metal and the salt. Deconvolution of the results in Fig. 5b are consistent with the separation.

CONCLUSIONS

1. In situ x-ray microprobe techniques enable detailed measurements to be made within pits and pores to explore changes in solution composition and processes taking place at electrode surfaces.

2. Within artificial pits where saturated solutions of dissolving stainless steel and salt layers develop, Br_2 forms at elevated potentials in bromide containing solutions. This contrasts with bromide free chloride solutions where no reaction, other than salt formation was observed.

3. At intermediate potentials the salt is replaced by small amounts of Br_2. At higher potentials copious amounts of Br_2 are continuously produced undermining the salt layer.

4. Br, being a heavier element acts as an x-ray marker for Cl, but only under limited conditions, as Br produces reactions not observed in the presence of chlorides alone.

ACKNOWLEDGMENTS

The authors gratefully acknowledge discussions with Grace Shea-Mc Carthy and Steven Sutton. The x-ray fluorescent microprobe measurements were carried at the Beamline X26A of the National Synchrotron Light Source at Brookhaven National Laboratory under Grants NASA NAG9 and NSF EAR86-18346. The work was performed under the auspices of the U.S. Department of Energy, Division of Materials Sciences, Office of Basic Energy Sciences under Contract No. DE-AC02-76CH00016.

REFERENCES

1. H. S. Isaacs and S.-M Huang, J. Electrochem. Soc., 143, L277 (1996).
2. H. S. Isaacs, J.-H. Cho, M. L. Rivers, R. S. Sutton, J. Electrochem. Soc., 142, 1111 (1995).
3. G. von Hevesey, Chemical Analysis by X-Ray and Its Applications, McGraw Hill, Inc., New York (1932)
4. B. Dziunilowski, Energy Dispersive X-Ray Fluorescence Analysis, Elsevier Science Publishing Co., Inc., New York (1989).
5. M. L. Rivers, S. R. Sutton and K. W. Jones, Synchronous Radiation News, 40(2), 23, (1991).
6. Corrosion Chemistry within Pits, Crevices, and Cracks. A. Turnbull, Eds., HMSO Books, London, 1987.
7. R. G. Kelly, This Symposium.

8. G. Salamat, G. A. Juhl, R. G. Kelly, "The Mechanism of Dissimilar Metal Crevice Corrosion in Superferritic Stainless Steel," Corrosion, 51, pp. 826-836 (1995).
9. K. R. Cooper, R. G. Kelly, "Sources of Variability in Cation Analyses for Exfoliation Corrosion Resistance Test," J. Chromatog. A., 740, pp. 183-90 (1996).
10. G. T. Gaudet, W. T. Mo, T. A. Hatton, J. W. Tester, J. Tilly, H. S. Isaacs, and R. C. Newman, AIChE Journal, 32, 949 (1986).
11. U. Steinsmo and H. S. Isaacs, J. Electrochem. Soc., 140, 643 (1993).
12. P. C. Pistorius and G. T. Burstein, Phil. Trans. R. Soc. Lond. A, 341, 531 (1992).
13. N. J. Laycock and R. C. Newman, Corros. Sci., in press.
14. G. S. Frankel, This Symposium.
15. Critical Factors in Localized Corrosion,. PV 92-9, G. S. Frankel and R. C. Newman, Eds., The Electrochemical Society, Pennington, NJ, (1992).
16. Critical Factors in Localized Corrosion II. PV 95-15, P. M. Natishan, R. G. Kelly, Pennington, NJ, (1995).
17. Passivity of Metals. R. P. Frankenthal and J. Kruger, Eds., The Electrochemical Society, Princeton, NJ, (1978).
18. R. -D. Grimm and D. Landolt, Corros. Sci., 36, 1847 (1994).
19. F. Hunkeler, A. Krolikowski and H. Bohni, Electrochim. Acta, 32, 615 (1987).
20. M. J. Danielson, J. Electrochem. Soc., 1326, (1988).
21. H. S. Isaacs. J. Electrochem. Soc., 120, 1456 (1973).
22. M. Pourbaix, "Atlas of Electrochemical Equilibria" National Association of Corrosion Engineers, Houston, TX,1974
23. N.Casillas, S. Charlebois, W.Smyrl, H. White, J. Electrochem. Soc., 141, 636 (1994).

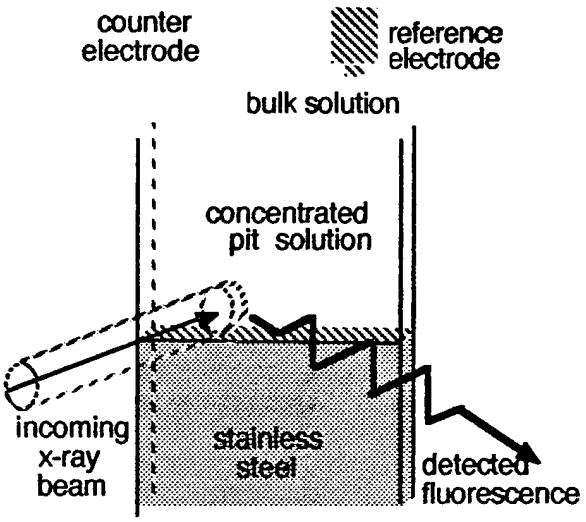

Figure 1. Schematic of the cell forming an artificial pit by dissolving back a stainless steel foil in a halide bulk solution.

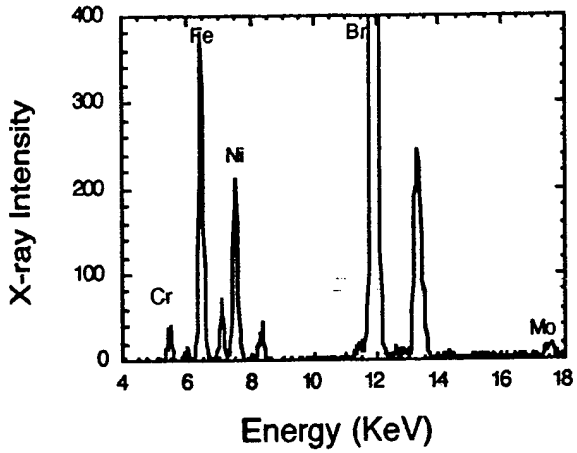

Figure 2 X-ray fluorescence spectrum from solution 20μm above an Fe alloy with 20% Ni, 12% Cr, and 5% Mo in a bromide containing solution.

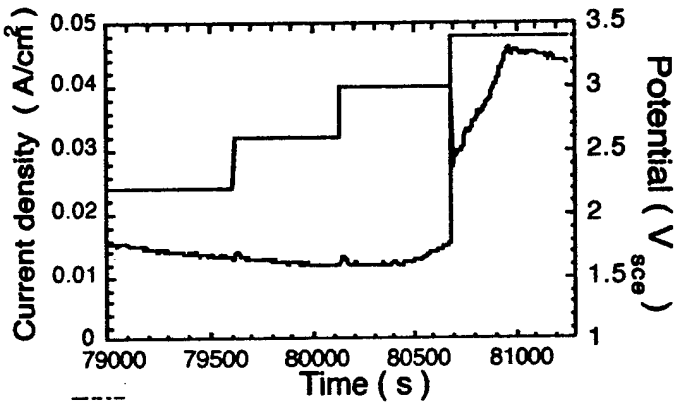

Figure 3. Variation of the potential and current with time for the Type 316 stainless steel artificial pit electrode approximately 0.7 mm deep during dissolution with a bulk solution of 1.0 M $LiCl_{0.75}Br_{0.25}$.

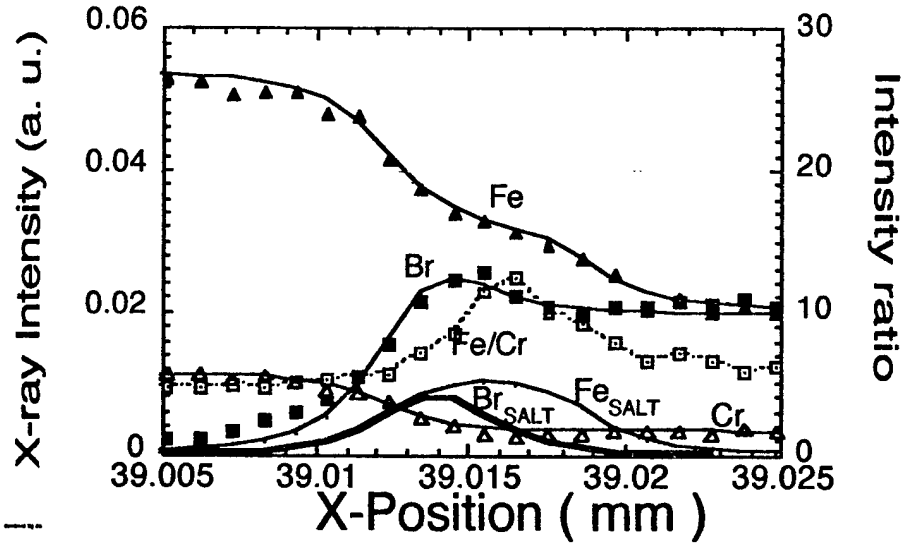

(a)

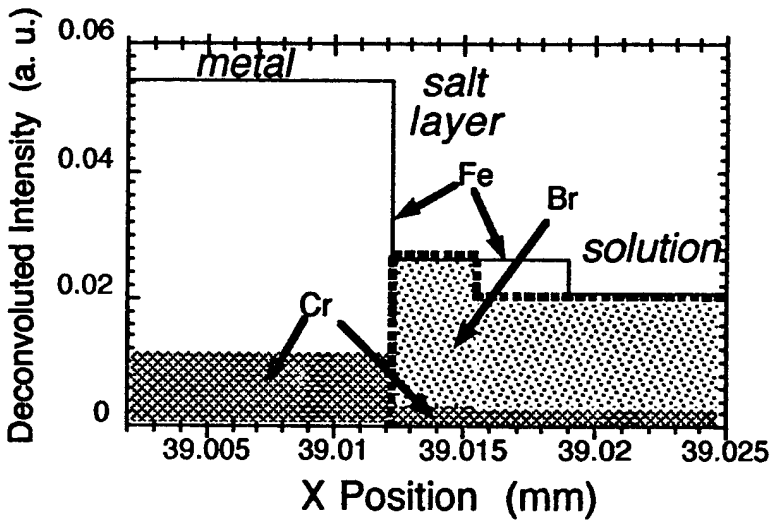

(b)

Figure 4. (a) Variations in fluorescence intensity with distance across a Type 316 stainless steel interface in an artificial pit in contact with saturated pit solution at 2.6 V_{sce}. The points are observed results. The broken line shows the variations in the Fe/Cr intensity ratio. (b) A deconvolution of the results in (a) for Fe, Cr and Br. The full lines in (a) are the convolution of the model of the interface in (b) and the shape of the x-ray beam.

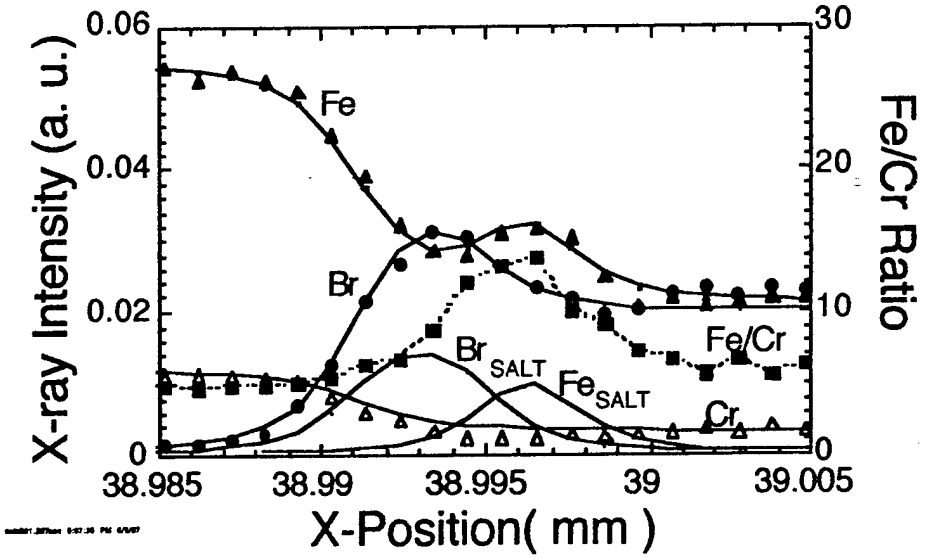

(a)

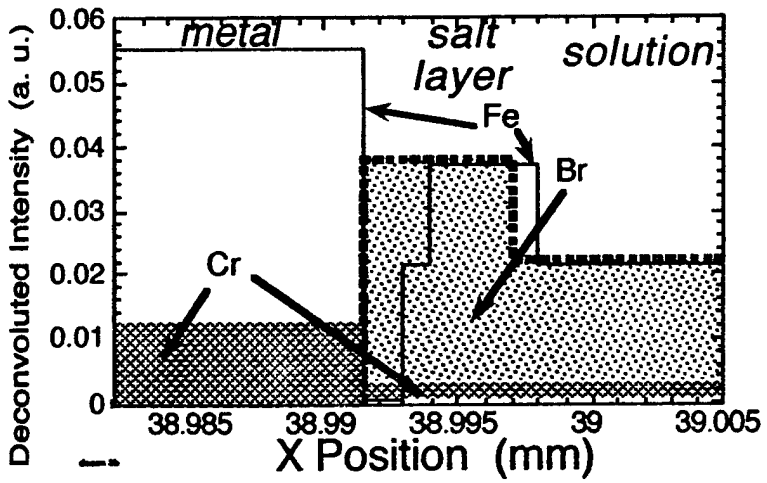

(b)

Figure 5. (a) Variations in fluorescence intensity with distance across a Type 316 stainless steel interface in an artificial pit in contact with saturated pit solution at 3.0 V_{sce}. The points are observed results. The broken line shows the variations in the Fe/Cr intensity ratio. (b) A deconvolution of the results in (a) for Fe, Cr and Br. The full lines in (a) are the convolution of the model of the interface in (b) and the shape of the x-ray beam.

Report Number (14) BNL--64624
CONF-970517--

Publ. Date (11) 199707
Sponsor Code (18) DOE/ER, XF
UC Category (19) UC-404, DOE/ER

DOE